23rd ABCM International Congress of Mechanical Engineering
December 6-11, 2015, Rio de Janeiro, RJ, Brazil

ANALYSIS OF HEAT TRANSFER COOLING RATE AND ITS EFFECT IN THE GTA ALUMINUM ALLOY WELDING

Elisan dos Santos Magalhães
Ana Lúcia Fernandes de Lima e Silva
Sandro Metrevelle Marcondes Lima e Silva
Heat Transfer Laboratory – LabTC, Institute of Mechanical Engineering – IEM, Federal University of Itajubá – UNIFEI, Campus Prof. José Rodrigues Seabra, Av. BPS, 1303, 37500-903, Itajubá, MG, Brazil.
elisanmagalhaes@hotmail.com, alfsilva@unifei.edu.br, metrevel@unifei.edu.br

Abstract. *An analysis of the heat transfer coefficient by convection and the emissivity in a GTA (Gas Tungsten Arc) welding process, on a 6060 T5 aluminum alloy is presented in this work. The authors' computational code was improved. In this software, an iterative BFGS (Broydon-Fletcher-Goldfarb-Shanno) inverse method was applied to minimize the amount of heat delivered to the plate when the appropriate sensitivity criteria were defined. The thermal properties were temperature dependent. The methodology was validated by accomplishing lab controlled experiments. Due to some experimental singularities the forced thermal convection induced by electromagnetic field and thermal-capillarity force could be disregarded. Significant examples of these singularities are the relatively small weld bead when compared to the sample size and the reduced time of welding process. An empirical correlation based on the local Nusselt number for flat plates was used to estimate the local heat transfer coefficient h. The presented method solved the thermal problem satisfactorily. The heat loss during the welding only by free convection proves to be more than 65% of overall cooling process.*

Keywords: *Inverse problems; Heat flux; Temperature estimation; GTAW process; Free convection; Thermal efficiency.*

1. INTRODUCTION

The GTA (Gas Tungsten Arc) welding process is largely used in industrial applications nowadays (Gonçalves *et al*., 2006). Due to its great welding quality and low equipment cost, this process is extensively applied to stainless steel, titanium alloy and nonferrous metals welds (Dong *et al*., 2011). In the GTA welding process, a tungsten electrode is protected by a flow of inert gas; argon is usually employed as well as helium, nitrogen, hydrogen or mixtures (Gonçalves *et al.,* 2010). The knowledge of the heat flux, temperature gradients and cooling process are thoroughly necessary for welding process studies. The thermal analysis is fundamentally based on models of heat transfer theory, which includes the following phenomena: Specific Heat, Latent Heat, Two Phase Regions, Moving Interfaces, Conservation of Energy, Fluid Mechanics, Conductivity, Contact Resistance, Radiation Emissivity and Convection (Goldak and Akhlaghi, 2005). Due to the high interaction level of those phenomena, since 1970s' several studies have been continuously accomplished to determine and improve the thermophysical properties of the weld bead (Shorshorov *et al*., 1973; Sluzalec, 1989; Sunar *et al*., 2006; Fallahi *et al*., 2011; Piekarska *et al*., 2011; Uday *et al*., 2012).

The weld quality depends on several parameters to control the temperature of the workpiece. For instance, the electric current and the torch speed are important factors of the GTA welding process (Li *et al*., 2012; Yadaiah and Bag, 2012). However, the heat losses play the major role in the weld quality. Consequently, the cooling process should be based on two important factors: convection and radiation. The natural cooling effect cannot be stopped. Indeed, the free or natural convection is caused by the action of the density gradients in conjunction with a gravitational field (Bejan and Krauss, 2012).

Several models were proposed for analysis of heat convection in welding. As an example, in Kou and Wang (1986), a three-dimensional model for a convection analysis in moving arc weld pool was presented. Murphy (2013) analyzed the convection and radiation heat-transfer through the presence of metal vapor in a gas-metal arc welding. Likewise, Marangoni effect has been largely used to model weld pool (Tsai and Kou, 1989; Xu *et al*., 2007; Fujii *et al*, 2008; Lu *et al*., 2008; Sándor *et al*., 2013).

In a previous study, Magalhães *et al*. (2015) used a constant convection coefficient to analyze the thermal model of a GTA aluminum alloy welding. The authors developed a software named "Inverse Heat Welding Problem 3D" (IHWP3D) based on a three-dimensional heat transfer transient model with moving heat source. The Specification Function technique (Beck *et al*., 1985) was used to estimate the heat flux applied on the workpiece by using experimental temperature data. The thermal field in any region of the plate or any time was determined with the estimated heat rate delivered to the workpiece. The theoretical temperatures were calculated from the heat diffusion equation, which was solved numerically in three-dimensional Cartesian coordinates by using the Finite Difference Method and the Implicit Euler Method for time discretization. The Modified Strongly Implicit (MSI) procedure

(Schneider and Zenan, 1981) was used for solving the system of algebraic equations. The temperature field was then obtained through the solution of the heat diffusion equation. The thermal excitation was a moving heat source in direction *x*. The remaining surfaces were subject to constant heat losses: convection, h = 20 W/m^{2}K, and radiation ε = 0.21.

In the present work, improvements on the previously mentioned methodology were performed. The new version of the code presents an analysis on the natural convection and radiation in a GTA aluminum process. Empirical correlations for horizontal and slope surfaces were used to calculate the convection heat transfer coefficient (Bergman *et al*., 2011). Also, the thermal conductivity, the thermal diffusivity and the emissivity are considered variable. An iterative BFGS (Broydon-Fletcher-Goldfarb-Shanno) inverse method was applied to minimize the amount of heat delivered to the plate when the appropriate sensitivities criteria are defined (Vanderplaats, 2005). The enthalpy method was applied to the three-dimensional thermal model (Al-Khalidy, 1997).

2. THEORETICAL FORMULATION

2.1 Direct problem

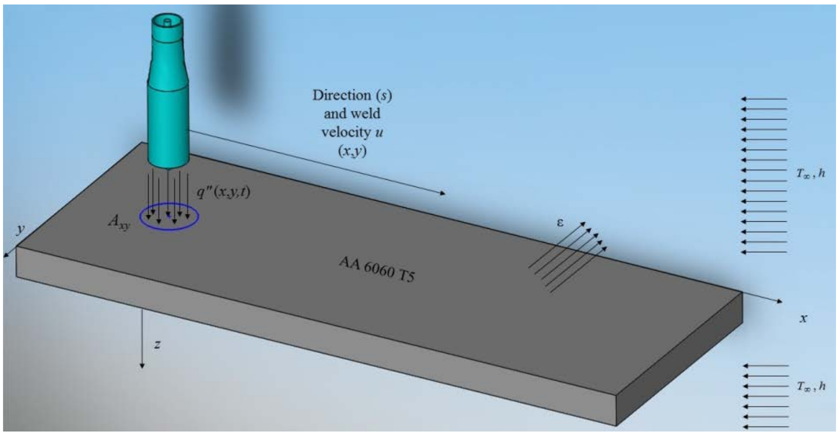

Figure 1: Scheme representation of the three-dimensional thermal welding process

The thermal model presented in Fig. 1 may be described by the transient three-dimensional diffusion equation with moving heat sources and phase change:

$$\frac{\partial}{\partial x}\left(k(T)\frac{\partial T}{\partial x}\right)+\frac{\partial}{\partial y}\left(k(T)\frac{\partial T}{\partial y}\right)+\frac{\partial}{\partial z}\left(k(T)\frac{\partial T}{\partial z}\right)=\frac{\partial H(T)}{\partial t}, \tag{1}$$

where $H(T)$ is the enthalpy function defined by Crank (1984).

The problem presented in Fig. 1 is subject to the boundary conditions of convection and radiation

$$-k(T)\frac{\partial T}{\partial \eta}=h(T)\left(T-T_\infty\right)+\sigma\cdot\varepsilon(T)\left(T^4-T_\infty^4\right) \tag{2}$$

where T is the calculated temperature, η is the normal direction, h is the heat transfer coefficient by convection, k the thermal conductivity, σ the Stefan-Boltzmann constant, ε the emissivity, T_∞ the room temperature and $q''(x,y,t)$ the unknown heat flux.

In the area defined by A_{xy}, the following boundary condition is applied:

$$-k(T)\frac{\partial T}{\partial z}=q''(x,y,t) \tag{3}$$

The initial condition of prescribed temperature is used for the entire domain as:

$$T(x,y,z,0)=T_0 \tag{4}$$

The solution of the temperature field is obtained through the numerical approximation of Eq. (1) by using the Finite Difference method. The linear system of algebraic equations is solved by using MSI – Modify Strongly Implicit procedure (Schneider and Zenan, 1981).

The heat flux $q(x,y,t)$ (see Fig. 1) is applied to a circular region and releases its energy continuously over the time as it moves with a constant velocity u positive in x direction:

$$q(x,y,t) = D(x,y,t) \times \left((x - u_x \cdot t)^2 + (y)^2 \right) \tag{5}$$

where u_x is the speed components in direction x and t is the time. The Gaussian or normal heat distribution $D(x,y,t)$ may be expressed according to Goldak and Akhalaghi (2005) as:

$$D(x,y,t) = M(t) \cdot e^{-C \cdot (x^2 + y^2)} \tag{6}$$

where x and y are the Cartesian coordinates, C is the distribution width coefficient. Coefficient C is directly related to the heat source width; a smaller diameter would lead to a more concentrated source, consequently a higher value of C (Goldak and Akhalaghi, 2005). $M(t)$ is the maximum heat flux in the center of the heat source. It could be determined through the following expressions:

$$M(t) = \frac{Cr^2 B(t)}{1 - e^{-Cr^2}} \tag{7}$$

where $B(t)$ is the heat input function from the BFGS inverse technique (Vanderplaats, 2005) and r the radius of the area A_{xy}.

2.2 Thermal model

Due to the temperature gradients in the air and the gravitational field, there is an induction of natural convection currents around the sample. The Nusselt number obtained from empirical correlations of the literature (Bergman *et al.*, 2011) was used to determine the convection coefficient h.

The cooling rate analysis is based on the experimental procedure and data from Magalhães *et al.* (2015). In that work, four t+ experimental conditions (2ms, 7ms, 11ms and 13ms) were tested and three experiments were carried out for each condition with the aim of assessing the repeatability of the estimated heat flux results. Four experimental temperatures were used to estimate the heat flux by using the BFGS technique. The temperatures were collected from four thermocouples fixed on the opposite side of the weld region. For each experiment, 482 temperature points were observed at a time interval, Δt, of 0.66 s. The welding speed was 62.5 mm/min. The mushy zone was delimited by the lowest temperature of solid-liquid transition, T_s = 615 °C and the highest temperature of solid-liquid transition, T_l = 655 °C (Toten and Macknzie, 2003). In the present work, the simulations were carried out using a new mesh to enhance the previous software (Magalhães *et al.*, 2015). The Cartesian mesh is non-uniform in x and y directions and uniform in coordinate z. It has an overall of 225.000 volumes. This mesh configuration maximizes the number of mesh points on the heated region (Fig. 2) where the temperature gradients are higher. The equations for the thermal conductivity k, the electrical resistivity λ, and the specific heat c_p were taken from fitting data points of Hatch (1984), McDonald (1967) and Jensen *et al.* (1980), respectively.

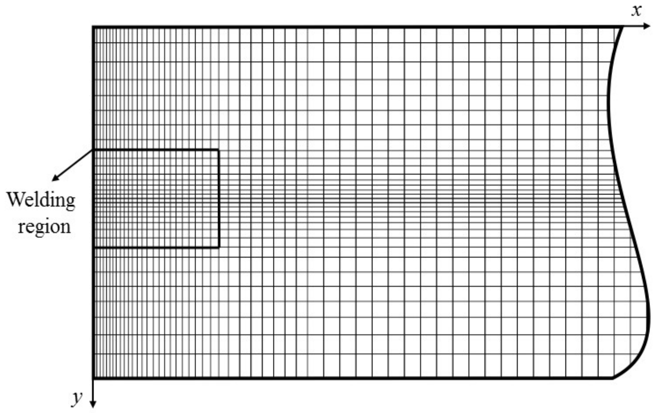

Figure 2: Non-uniform *xy* Cartesian mesh applied in simulation.

Table 1 presents the values of the calculated property values for specific temperatures.

Table 1: Values of temperature-dependent thermal properties.

T K	k W/mK	λ $\Omega \cdot cm$	c_p $J/kg \cdot K$	ρ kg/m^3	ε
300	237	2.80	902	2368	0.20
400	240	4.07	956	2368	0.22
600	231	6.61	1042	2368	0.28
800	218	9.15	1143	2368	0.34
933	208	10.95	1260	2368	0.36
1000	93	25.14	1126	2345	0.40
1200	99	28.08	1126	2304	0.41

3. RESULT ANALYSIS

Figure 3 presents a comparison between the temperature signals measured by thermocouples T_1, T_2, T_3 and T_4. The respective numerical temperature was calculated from the estimated heat flux through BFGS (Broydon-Fletcher-Goldfarb-Shanno) technique, for the welding conditions $t+$ = 2ms, $t+$ = 7ms, $t+$ = 11ms and $t+$ = 13ms. An increase in the temperature may be observed with the increase of positive polarity ($t+$).

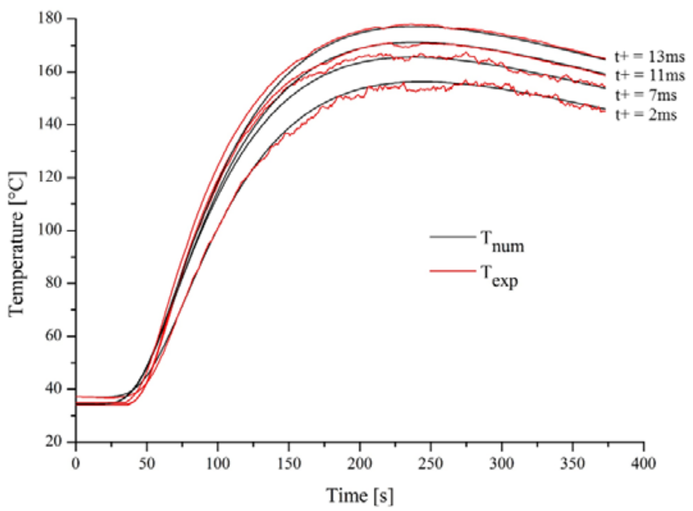

Figure 3: Evolution of the experimental and numerical temperatures for different $t+$ conditions.

Table 2 presents the average heat rate for the four experimental conditions tested.

Table 2: Average heat rate for each test.

Adjusted (t+)(ms)	Obtained (t+) (ms)	Total power (W)	Estimated useful power (W)	Thermal efficiency (%)
2	2.2	2037	926.2	45.5
7	6.9	2181	991.3	45.5
11	11.3	2335	1071.4	45.9
13	13.3	2702	1253.6	46.4

The Equations from Bergman *et al.* (2011) were used to calculate Nu_l and h in any position on the plate. Figure 4 presents the average Nu_m profile. The dimensionless number Gr_l / Re_l^2 remained much higher than one in all calculated points; consequently, the problem could be treated as pure free convection (Bergman *et al.*, 2011).

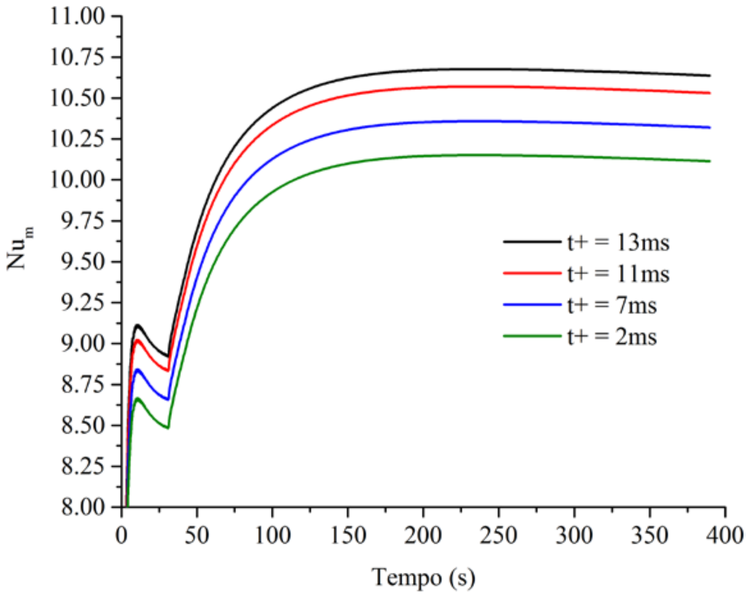

Figure 4: Average Nu_m

Figure 5 shows the average heat transfer coefficient for the four *t+* welding conditions. It could be observed that the average heat transfer coefficient achieves the maximum value when the GTA torch is turned off. After this step of time, it starts to decrease slowly.

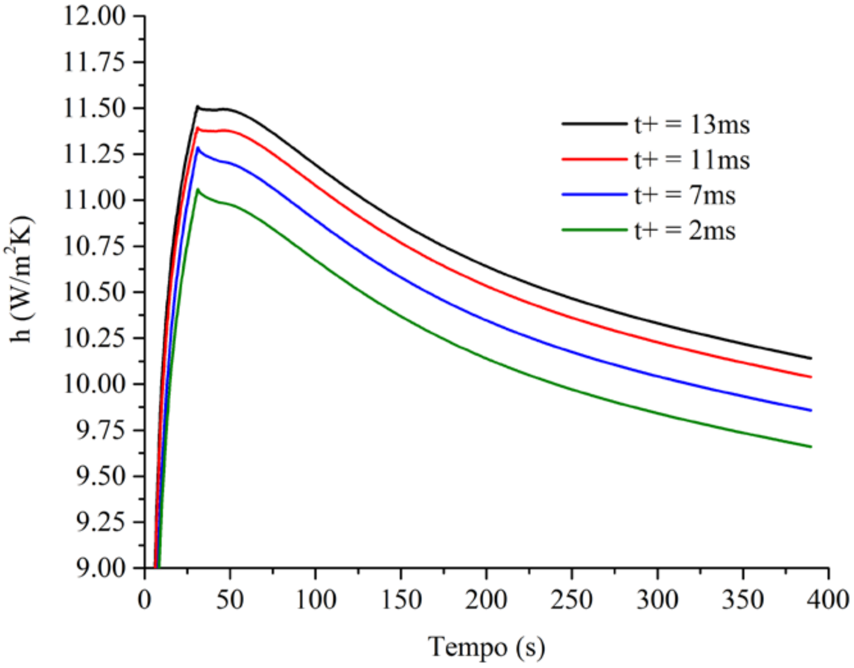

Figure 5: Average heat transfer coefficient.

The heat transfer rate lost by convection when a variable heat transfer coefficient is considered must be pointed out. By determining the average temperature and the average heat transfer coefficient, the study showed that the variable heat transfer coefficient represents almost 65% of the overall heat transfer loss rate independently of *t+* welding condition. Figure 6 presents the percentage of heat loss by natural convection and radiation versus the time. Although the natural convection represents a big part of the cooling process, the heat loss by radiation affects significantly the cooling process in the GTA aluminum welding. As the matter of fact, the radiation losses while the torch still on represents almost 70% of the overall heat cooling.

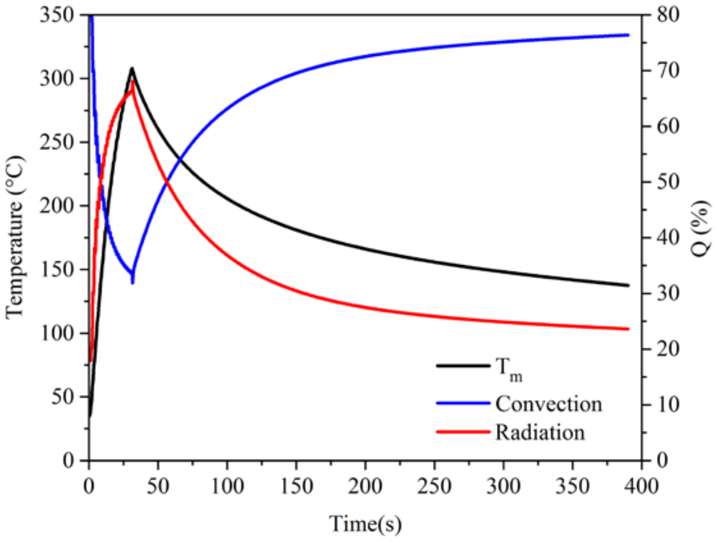

Figure 6: Average temperature and percentage of heat loss due to natural convection and radiation for t+ = 13ms.

Figures 7 and 8 present the two-dimensional distribution of the heat transfer coefficient by convection for four time steps for the welding condition *t*+ = 7ms and *t*+ = 13ms, respectively. It may be seen that the convection coefficient reaches its highest value just before the torch is turned off. After 33s, the heat transfer coefficient tends to stabilize at approximately 10W/m^2.K (Figure 5). This value is obtained due to the fact that after this time the heat delivered by the GTA torch is well distributed on the plate. Consequently, all surface points tend to have the same temperature and heat transfer coefficient.

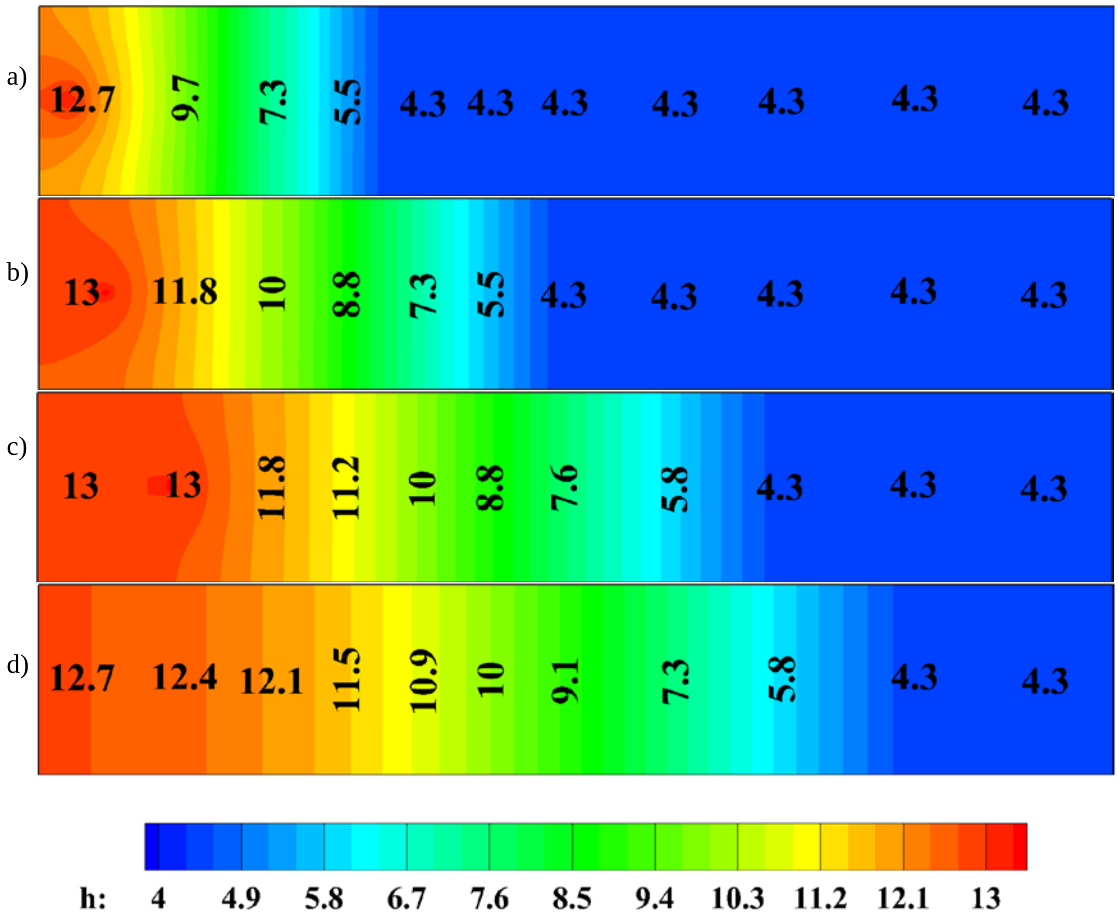

Figure 7: Evolution of the heat transfer coefficient, *h* W/m^2.K, at instants: a) 6.6s, b) 15.0s c) 26.4s and d) 33.0s for *t*+ = 7.0ms

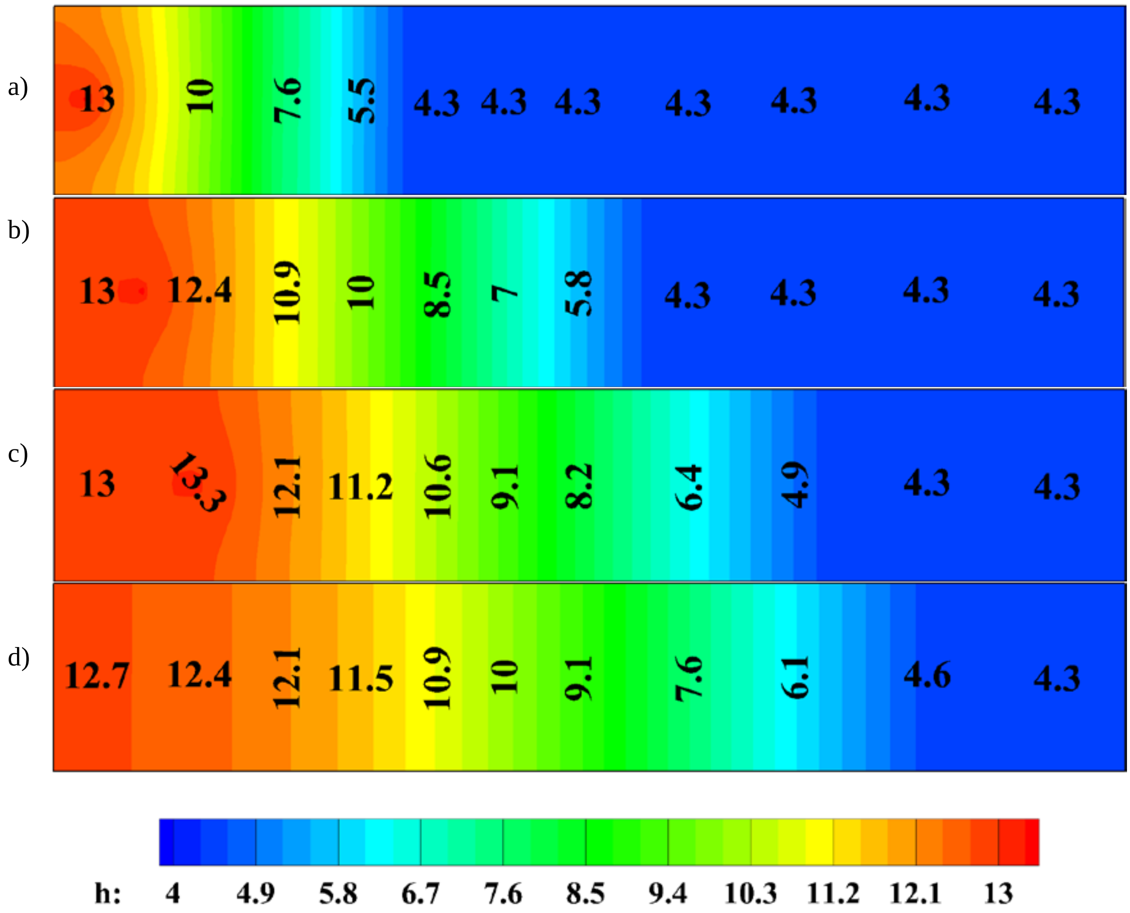

Figure 8: Evolution of the heat transfer coefficient, h W/m^2.K, at instants: a) 6.6s, b) 15.0s c) 26.4s and d) 33.0s for t+ = 13.0ms

4. CONCLUSIONS

This paper presented an analysis of the cooling rate (heat transfer rate lost) by convection and radiation on an aluminum 6060-T5 plate, under GTA welding process, from the observation of the thermal fields calculated by a homemade C++ code. The free convection effect is an important factor in heat transfer losses for the case analyzed. In fact, it represents more than 65% of overall heat losses. However, the radiation losses are significantly while the GTA torch stills on. Consequently, this paper could be used to support a study to minimize the Heat Affected Zone (HAZ) effect in aluminum alloy welding. Consequently, it should improve the GTAW process quality. The similarity between the experimental and calculated parameters validated and proved the efficiency of the software developed when applied to the resolution of thermal problems in welding.

5. ACKNOWLEDGEMENTS

The authors would like to thank CNPq, CAPES and FAPEMIG for their financial support.

6. REFERENCES

Al-Khalidy, N., 1997. “Application of optimization methods for solving inverse phase change problems”. *Numerical Heat Transfer-part B*, pp. 477 – 497.

Beck, J.V., Blackwell, B., Clair, C.St., 1985. *Inverse Heat Conduction: Ill-posed Problems*. Wiley Interscience Publication, New York.

Bejan, A. and Kraus, A.D., 2003. *Heat Transfer Handbook.* John Wiley & Sons, 1481p.

Bergman, T. L., Lavine, A. S., Incropera, F. P., DeWitt, D. P., 2011. *Fundamentals of Heat and Mass Transfer*, John Wiley & Sons, 7th ed., USA, 1076 p.

Crank, J., 1984. “Free and moving boundary problems”, *Claredon Press*, Oxford University Press, New York.

Davisson C. and Weeks Jr., J.R.. 1924. “The relation between the total thermal emissive power of a metal and its electrical resistivity”, *Journal of the Optical Society of America*, Vol. 8, 25p.

Dong, W., Lu, S., Li, D., Li, Y., 2011. "GTAW liquid pool convections and the weld shape variations under helium gas shielding". *International Journal of Heat and Mass Transfer*, vol. 54, pp. 1420-1431.

Fallahi, A., Jafarpur, K., Nami, M.R., 2011. "Analysis of welding conditions based on induced thermal irreversibilities in welded structures: Cases of welding sequences and preheating treatment", *Scientia Iranica Transactions B: Mechanical Engineering*, vol. 18, pp. 398-406.

Fujii, H., Sato, T., Lu, S., Nogi, K., 2008. "Development of an advanced A-TIG (AA-TIG) welding method by control of Marangoni convection". *Materials Science and Engineering A*, vol. 495, pp 296-303.

Goldak, J. A. and Akhlaghi, M., 2005. *Computation Welding Mechanics.* Springer, 2005.

Gonçalves, C.V., Carvalho, S.R., Guimarães, G. 2010. "Application of optimization techniques and the enthalpy method to solve a 3D-inverse problem during a TIG welding process". *Applied Thermal Engineering*, vol. 30, pp. 2396-2402.

Gonçalves, C.V., Vilarinho, L.O., Scotti, A., Guimarães, G., 2006. "Estimation of heat source and thermal efficiency in GTAW process by using inverse techniques", *Journal of Materials Processing Technology*, vol. 172, pp. 42-51.

Hatch, J. E., 1984. *Aluminum properties and physical metallurgy*. ASM International.

Kou, S. and Wang, Y. H., 1986. "Computer Simulation of Convection in Moving Arc Weld Pools". *Metallurgical and Materials Transactions A*, vol. 17, pp 2271-2277.

Jensen, J.E., Tuttle, W.A., Stwart, R.B., Brechna, H., Prodell, A.G., 1980. *Selected Cryogenic Data Notebook*. Brookhaven National Laboratory, United States Department of Energy, Vol. II.

Li, D., Lu, S., Dong, W., Li, D., Li, Y., 2012. "Study of the law between the weld pool shape variations with the welding parameters under two TIG process". *Journal of Materials Processing Technology*, vol. 212, pp. 128-136.

Lu, S., Fujii, H., Nogi, K., 2008. " Marangoni convection and weld shape variations in He-CO_2 shielded gas tungsten arc welding on SUS304 stailess stell". *Journal of Materials Science*, vol. 43, pp. 4583-4591.

Magalhães, E.S., Carvalho, S.R., Lima e Silva, A.L.F., Lima e Silva, S.M.M. 2015. "The use of non-linear inverse problem and enthalpy method in GTAW process of aluminum", *International Communications in Heat and Mass Transfer*, vol. 66, pp. 114-121.

McDonald, R.A., 1967. "Enthalpy, Heat Capacity, and Heat of Fusion of Aluminum from 336° to 1647° K", *Journal of Chemical Engineering Data*, Vol. 12, pp. 115-118.

Murphy, A.B., 2013. "Influence of metal vapour on arc temperatures in gas-metal arc welding: convection versus radiation", *Journal of Physics D: Applied Physics*, vol. 46, 10pp.

Piekarska, W., Kubiak, M., 2011. "Three-dimensional model for numerical analysis of thermal phenomena in laser-arc hybrid welding process". *International Journal of Heat and Mass Transfer*, vol. 54, pp. 4966-4974.

Ramanathan, K.G., and Yen, S.H., 1977. "High-temperature emissivities of copper, aluminum, and silver". *Journal of the Optical Society of America*, Vol. 67, pp 1-7.

Sándor, T., Mekler, C., Dobranszky, J., Kaptay, G., 2013. "An improved theoretical model for a A-TIG welding based on surface transition and reverse Marangoni Flow". *Metallurgical and Materials Transaction A*, vol. 44, 11 p.

Schneider, G.E. and Zenan, M. 1981. "A Modified strongly implicit procedure for the numerical solution of field problems", Numerical Heat Transfer, 4:1, pp. 1-19.

Shorshorov, M. Kh., Antipov, V. I., Kudinov, E. D., Mikhaleva, É. I., 1973. "Effect of the thermal cycle in welding on the structure and phase composition of the heat-affected zone in maraging steel". *Metal Science and Heat Treatment*, vol. 15, 2p.

Sluzalec, A., 1989. "An analysis of thermal phenomena in electromagnetic field during electroslag welding". Computer & Fluids, vol. 17, pp. 411-418.

Sunar, M., Yilbas, B. S., Boran, K., 2006. "Thermal and stress analysis of a sheet metal in welding". Journal of Materials Processing Technology, vol. 172, pp. 123-129.

Tsai, M.C. and Kou, S., 1989. "Marangoni convection in weld pools with a free surface". *International Journal for Numerical Methods in Fluids*, vol. 9, pp. 1503-1516.

Toten, E.F. and Macknzie, D. S., 2003. *Handbook of Aluminum – Physical Metallurgy and Process*. Marcel Dekker, Inc, Vol 1, 1309p.

Uday, M.B., Ahamad Fauzi, M.N., Zuhailawati, H., Ismail, A.B., 2012. "Thermal analysis of friction welding process in relation to the welding YSZ-alumina composite and 6061 aluminum alloy". *Applied Surface Science*, vol. 258, pp 8264-8272.

Vanderplaats, G. N., 2005. *Numerical optimization techniques for engineering design*. McGraw Hill USA, 4th edition, 465 p.

Xu, X.L., Dong, Z.B., Wei, Y.H., Yang, C.L., 2007. "Marangoni convection and weld shape variation in A-TIG welding process". *Theoretical and Applied Fracture Mechanics,* vol. 48, pp. (178-186).

Yadaiah, N. and Bag, S., 2012. "Effect of heat source parameters in thermal and mechanical analysis of linear GTA welding process", *ISIJ International*, vol. 52, pp. 2069-2075.

7. RESPONSIBILITY NOTICE

The authors are the only responsible for the printed material included in this paper.